Eur. Phys. J. B **26**, 467–471 (2002)
DOI: 10.1140/epjb/e20020115

THE EUROPEAN PHYSICAL JOURNAL B
EDP Sciences

Transport properties of $La_{1-x}Ca_xMnO_3$ ($0.5 \leq x < 1$)

H.-D. Zhou, R.-K. Zheng, G. Li, S.-J. Feng, F. Liu, X.-J. Fan, and X.-G. Li[a]

Structure Research Laboratory, Department of Materials Science and Engineering, University of Science and Technology of China, Hefei 230026, PR China

Received 4 January 2002 and Received in final form 28 January 2002

Abstract. The transport properties of the $La_{1-x}Ca_xMnO_3$ ($0.5 \leq x < 1$) system in magnetic fields up to 14 T were studied. We found that the relationship between the charge ordering temperature T_{CO} and Mn^{4+} content $n_{Mn^{4+}}$ obeys the formula $T_{CO}/T_{max} = 1 - a(n_{Mn^{4+}} - n_0)^2$, here n_0 and a are constants and T_{max} is the maximum of T_{CO}. For $x = 0.65$, T_{CO} arrives at the maximum value of 249.5 K in zero magnetic field, while the charge ordered (CO) state is most stable around $x = 0.75$. For $x = 0.5$ when $H < 6$ T the resistivity displays Mott's variable-range hopping (VRH) behavior, when $6 < H < 12$ T it is suggested that two kinds of conduction mechanism, *i.e.*, VRH and magnetic polarons, coexist in the material, and when $H > 12$ T the resistivity shows metallic-like behavior and the transport mechanism is attributed to coexistence of magnetic polarons and free carriers. For $x = 0.95$, the conduction mechanism accords with the coexistence of VRH and magnetic polarons.

PACS. 72.20.Ht High-field and nonlinear effects – 72.60.+g Mixed conductivity and conductivity transitions

1 Introduction

Currently, a large fraction of the work on mixed-valance manganites with the perovskite structure focuses on intermediate bandwidth materials, especially the $La_{1-x}Ca_xMnO_3$ system, since they present the largest negative colossal magnetoresistance (CMR) effects. For a broad doping range in $La_{1-x}Ca_xMnO_3$, $0.2 \leq x < 0.5$, there is an insulating-metallic (IM) transition associated with a paramagnetic (PM)-ferromagnetic (FM) transition, which has been traditionally explained in terms of the double exchange (DE) mechanism [1]. However recently detailed work has shown that DE alone is insufficient to account for the rich variety of phenomena found in these compounds, such as the charge ordered (CO) state in the region from $x = 0.50$ to $x = 0.87$ and other perovskite structure manganites [2–6]. The CO state at $x = 0.50$ was already described by Wollan and Koehler as a CE-state in 1955 [7]. Recently, a considerable amount of work has confirmed the coexistence of the FM and CO states. For example, the work by Chen and Cheong [8] and Radaelli *et al.* [9] using electron and X-ray diffraction experiments manifested this coexistence in a narrow temperature window of $La_{0.5}Ca_{0.5}MnO_3$. Further studies [10–12] showed that this mixture of FM and CO phases arises from an inhomogeneous spatial mixture of incommensurate charge-ordered and ferromagnetic charge-ordered microdomains, with a size of 20–30 nm. Roy *et al.* [13,14] analyzed magnetization, resistivity, and specific heat data, and concluded that in a narrow region of hole densities centered at $x = 0.5$ two types of carriers coexisted: localized and free, and at high magnetic field the CO state can collapse to a metallic state. For $x > 0.50$, the CO state seems to become more stable. For example [14,15], for $x = 0.55$ a field of 9 T is not high enough to destabilize the CO state, and for $x = 0.65$ a 12 T field is not sufficient to induce the metallic state. For $0.87 < x < 1$, there is ferromagnetic-like order, which can be denoted as canted anti-ferromagnetic (CAF) state [16]. Some work shows that in this state magnetization is most enhanced and negative magnetoresistance is obvious [16,17]. Despite all these works about $0.50 \leq x < 1$, how the CO and CAF states behave in high magnetic fields with increasing x, such as the magnetic field dependencies of T_{CO} and CAF temperature T_{CAF}, is not very clear. Furthermore how the transport mechanism changes with the application of magnetic field in CO and CAF states is also unclear.

In this paper, the transport properties for $La_{1-x}Ca_xMnO_3$ ($0.50 \leq x < 1$) in magnetic fields up to 14 T were studied and the conduction mechanism is discussed.

2 Experimental

Polycrystalline samples of $La_{1-x}Ca_xMnO_3$ ($0.50 \leq x < 1$) were prepared by a standard solid-state reaction method. A stoichiometric mixture of high purity La_2O_3 (baked above 800 °C for 2h), $CaCO_3$, and MnO_2 was ground

[a] e-mail: lixg@ustc.edu.cn

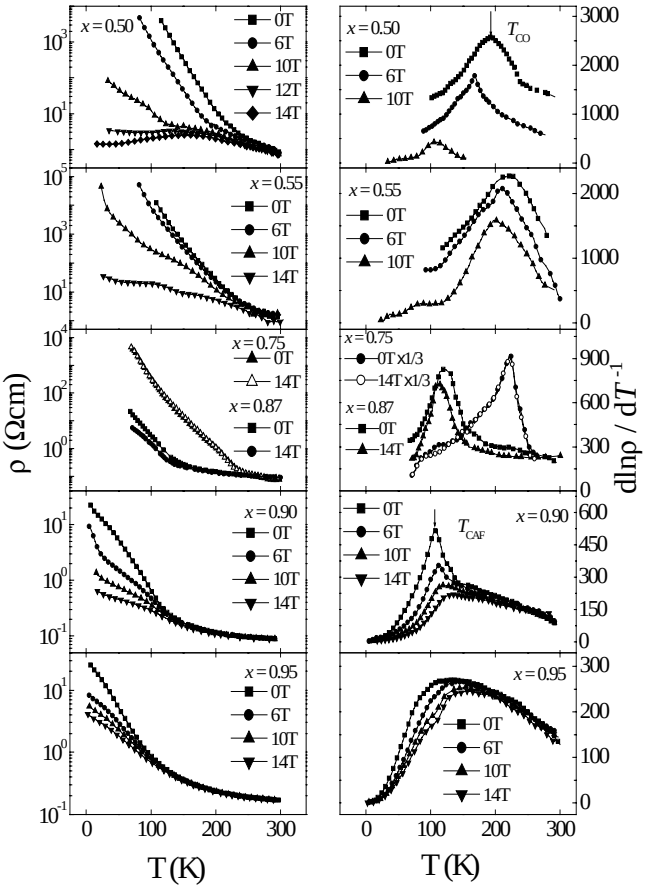

Fig. 1. Temperature dependencies of resistivity (ρ) and its logarithmic derivative, $\mathrm{d}\ln\rho/\mathrm{d}T^{-1}$, in different magnetic fields for $x = 0.5$, 0.55, 0.75, 0.87, 0.90, and 0.95.

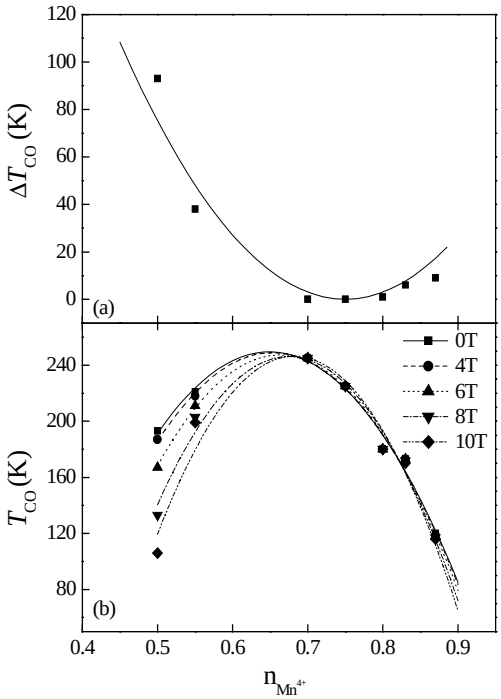

Fig. 2. (a) The relation between Mn^{4+} content and ΔT_{CO} for $0.50 \leq x \leq 0.87$. The solid line is a guide for eyes; (b) Variations of T_{CO} with Mn^{4+} content in different magnetic fields for $0.50 \leq x \leq 0.87$. The symbols are experimental data and the lines are fitted results using equation (1).

and calcined at 1200 °C for 24 h. The reactant was reground intermediately and pressed into pellets for sintering at 1300 °C for 24 h, then was cooled down to room temperature in the furnace. The powder X-ray diffraction patterns were recorded by a MacScience MAXP18AHF diffractometer using Cu K_α radiation. The XRD patterns show that all the samples are of single phase. The resistivity was measured by a standard four-probe technique heating to the room temperature at a rate of 2 K/min.

3 Result and discussion

Figure 1 shows the temperature dependencies of resistivity ($\rho \sim T$) and $\mathrm{d}\ln\rho/\mathrm{d}T^{-1} \sim T$ curves for $La_{1-x}Ca_xMnO_3$ ($x = 0.5$, 0.55, 0.75, 0.87, 0.90, and 0.95) in different magnetic fields (H) up to 14 T. T_{CO} and T_{CAF} are determined from the peak temperatures of the $\mathrm{d}\ln\rho/\mathrm{d}T^{-1} \sim T$ curves [18]. For $x = 0.75$ the resistivity does not change even when $H = 14$ T, but all other resistivities become smaller with the application of H when $T < T_{CO}$ (for $0.5 \leq x \leq 0.87$) and $T < T_{CAF}$ (for $x = 0.90$ and 0.95). Note that for $x = 0.5$, the resistivity shows a metallic like behavior as $H > 12$ T.

Figure 2a shows the relation between the Mn^{4+} content and $\Delta T_{CO}(\Delta T_{CO} = T_{CO}(0\,\mathrm{T}) - T_{CO}(14\,\mathrm{T})$. When $x < 0.75$, ΔT_{CO} decreases with increasing Mn^{4+} content, but when $x > 0.75$, ΔT_{CO} increases with increasing Mn^{4+} content. It implies that the CO state is most stable at $x = 0.75$. The Mn^{4+} content dependencies of T_{CO} for $H = 0$, 4, 6, 8, and 10 T are shown in Figure 2b. It is interesting that the relation between T_{CO} and Mn^{4+} content can be described as:

$$T_{CO}/T_{max} = 1 - a(n_{Mn^{4+}} - n_0)^2 \qquad (1)$$

where $n_{Mn^{4+}}$ is the Mn^{4+} content, n_0 is the content of Mn^{4+} when $T_{CO} = T_{max}$, and a is a constant, which is similar to the relation between T_C of high T_C-superconductor and carrier density n [19,20]. As can be seen from Figure 2b, the calculated results (lines) using equation (1) fit our experimental data (symbols) well. It is noted that at zero field $n_0 = 0.65$ and $T_{max} = 249.5$ K. With increasing magnetic fields n_0 increases and T_{max} decreases slightly. For $n_0 = 0.65$ the CO state is not the strongest and its T_{CO} will shift to low temperature region due to the suppression of the CO state in magnetic fields. Then T_{max} will decrease and may appear at a n_0 with a more stable CO state with increasing magnetic fields. So it is reasonable that n_0 increases towards 0.75 where the CO state is the strongest, in fact when $H = 10\,\mathrm{T}, n_0 = 0.68$ and $T_{max} = 246.5$ K.

The magnetic field dependencies of T_{CAF} for $x = 0.9$ and 0.95 are contrary to that of T_{CO} for $0.5 \leq x \leq 0.87$.

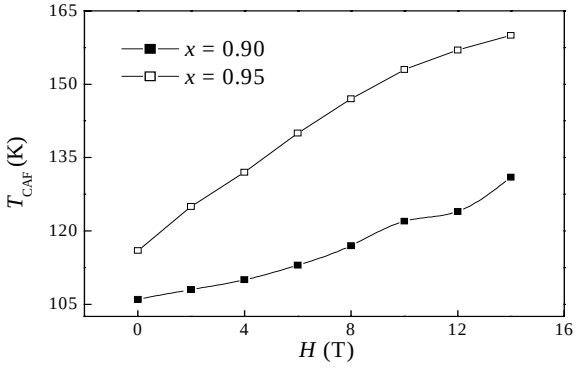

Fig. 3. The magnetic field dependencies of T_{CAF} for $x = 0.90$ and 0.95.

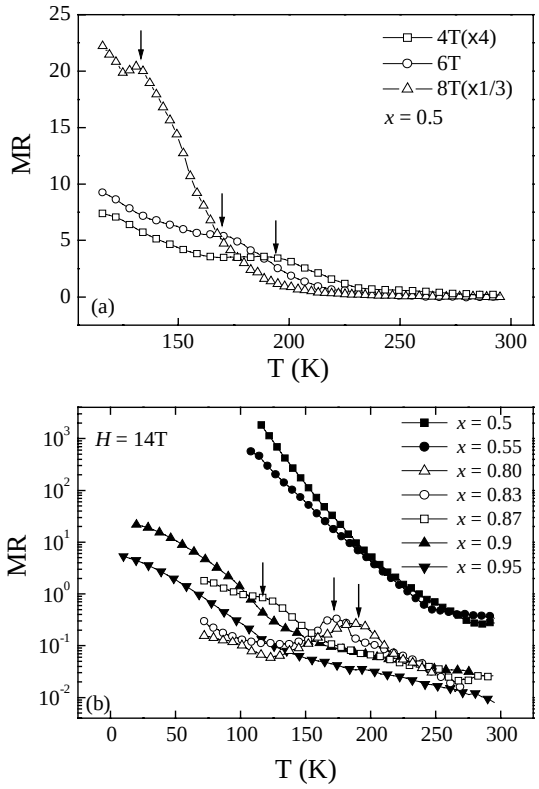

Fig. 4. (a) Temperature dependencies of MR for $x = 0.5$ when $H = 4$, 6, and 8 T; (b) Temperature dependencies of MR when $H = 14$ T for $0.50 \leq x \leq 0.95$.

T_{CAF} shifts to the high temperature region with increasing magnetic fields as shown in Figure 3. It may be due to that the ferromagnetic-like order in the CAF state is strengthened by magnetic fields.

The MR *vs.* T curves are plotted in Figure 4. Here the MR is defined by $\Delta\rho/\rho = [\rho(0) - \rho(H)]/\rho(H)$, $\rho(0)$ and $\rho(H)$ are the resistivity values in zero and a certain magnetic field, respectively. As shown in Figure 4a, for $x = 0.50$, when $H = 4$, 6, and 8 T the MR curves have peaks at 190, 170, and 131 K, respectively. However, the MR curve at 14 T rises steeply with decreasing temperature and does not have such a peak, suggesting that the transport mechanism for $x = 0.5$ in high magnetic fields is

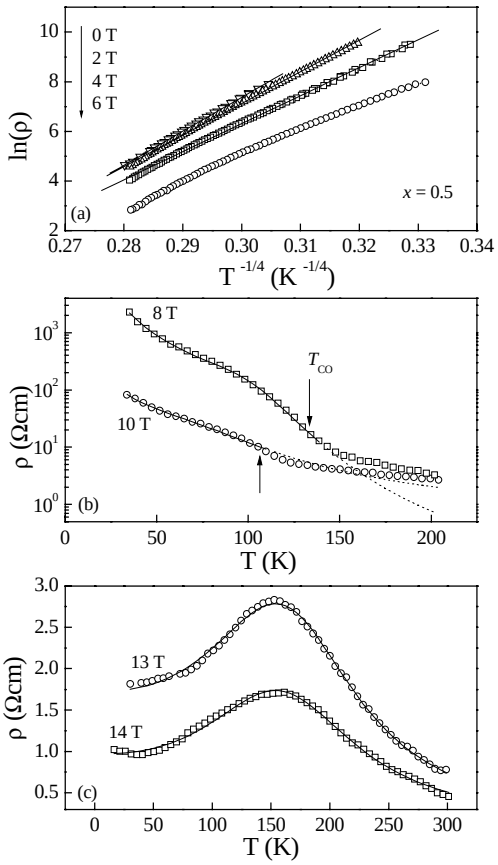

Fig. 5. (a) $\ln(\rho)$ *versus* $T^{-1/4}$ in different magnetic fields for $x = 0.5$. (b) Temperature dependencies of resistivity for $x = 0.5$ when $H = 8$ and 10 T. (c) Temperature dependencies of resistivity for $x = 0.5$ when $H = 13$ and 14 T. (The symbols are experimental data and the lines are the fitting results.)

different from that in low magnetic fields. The MR curves of 14 T for $x = 0.80$, 0.83, and 0.87 (Fig. 4b) also have the peaks at 185, 173, and 117 K, respectively. All these peak temperatures for different compositions are around their own T_{CO}. These results mean that the charge localization around T_{CO} is sensitive to magnetic fields.

In order to analyze the transport properties more clearly, we replotted the $\rho \sim T$ curves for $x = 0.5$ as $\ln\rho \sim T^{-1/4}$ in Figure 5a. It is found that when $H = 0$, 2, and 4 T, the experimental data at low temperatures ($T < 160$ K) show linear dependencies quite well, which suggests that the low-temperature resistivity accords with Mott's variable-range hopping (VRH) model [21], namely

$$\rho_{\mathrm{CO}} = \rho_0 \exp(T_0/T)^{1/4}. \tag{2}$$

However when $H = 6$ T, the experimental data deviate from the linear behavior as shown in Figure 5a, which is probably caused by the interaction between ferromagnetic (FM) clusters at high magnetic fields. The existence of FM clusters in $La_{0.5}Ca_{0.5}MnO_3$ has been confirmed by many other experiments [9–14]. These FM clusters are associated with the lattice distortion (small polaron). For larger magnetic fields, the short-range FM interactions

among them can induce magnetic polarization [22] and the size of FM clusters will increase. So the conduction between the FM clusters can be understood as the conduction from magnetic polarons: charge carriers accompanied by a localized (and magnetically polarized) distortion of the surrounding crystal lattice [23], which are universally proposed as the hopping motion of small polarons [24,25] and defined as $\rho_{\rm FM} = AT\exp(E/k_{\rm B}T)$ [21]. Since in the material the FM and CO clusters coexist and constitute a parallel connection in the temperature region below $T_{\rm CO}$ in high magnetic fields, two different kinds of conduction mechanism: VRH and magnetic polarons coexist in the material and the resistivity below $T_{\rm CO}$ can be described by the following formula:

$$\rho = \frac{\rho_{\rm FM}\ \rho_{\rm CO}}{\rho_{\rm FM} + \rho_{\rm CO}}\ . \tag{3}$$

We fitted the $\rho \sim T$ curves at fields 8 and 10 T, and the results are plotted as lines in Figure 5b. It can be seen that the lines are in good agreement with the experimental data (open circles) below $T_{\rm CO}$. The value of T_0 for $x = 0.5$ decreases with increasing magnetic fields as shown in Figure 7. In the theory of VRH, $T_0 \propto \alpha^3/k_{\rm B}N(E_{\rm F})$, where α^{-1} is the localization length, $k_{\rm B}$ is the Boltzmann constant, and $N(E_{\rm F})$ is the density of localized states at Fermi level. It is supposed that the change of $N(E_{\rm F})$ with applied magnetic fields could not account for the great decrease of T_0. The decrease of T_0 implies the increase of localization length α^{-1} which leads the delocalization. The abrupt drop of T_0 at 8 T shows that the growth of FM clusters suppresses the CO state or strengthens the delocalization efficiently.

When $H > 12$ T, the volume fraction of the FM clusters is so large that the clusters connect with each other, which results in the collapse of the CO state and the system shows metallic like properties. It is assumed that the conduction of the metallic region is from a small population of free carriers and the resistivity follows $\rho_{\rm M} = A + BT^{2.5}$, where A and B correspond to scattering by defects, and by a combination of phonons, electrons, and spin fluctuations and the exponent of 2.5 is an empirical fit [26]. In this form, the total resistivity of the material is due to the parallel conduction of $\rho_{\rm FM}$ and $\rho_{\rm M}$, so ρ can be written as

$$1/\rho = 1/(A + BT^{2.5}) + \frac{C}{T}\exp[-(E/k_{\rm B}T)]. \tag{4}$$

This equation fits the resistivity with $H = 13$ and 14 T well, as shown in Figure 5c.

For $x = 0.95$, the experimental data below $T_{\rm CAF}$ can be fitted well using equation (3), as shown in Figure 6. So it is suggested that the conduction of the ferromagnetic-like order in the CAF state is also dominated by magnetic polarons and the background accords with VRH model. Note that T_0 (shown in Fig. 7) is smaller than that for $x = 0.5$ and decreases dramatically with increasing magnetic fields. The small value of T_0 implies that in the CAF state the localization is weaker than that in the CO state. The sharp decrease of T_0 with increasing magnetic fields also means that the localization length increases rapidly while the delocalization is greatly strengthened. This may be the reason for the obvious negative magnetoresistance in the CAF state for $x = 0.95$.

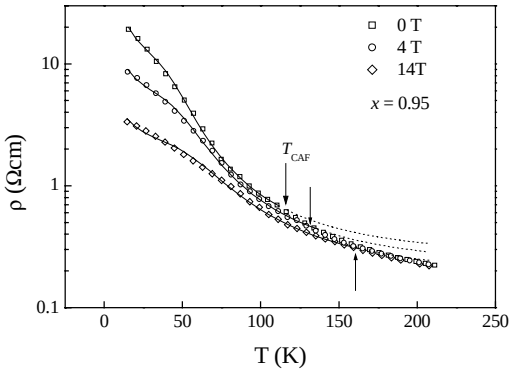

Fig. 6. Temperature dependencies of resistivity in different magnetic fields for $x = 0.95$. The symbols are experimental data and the lines represent the fitting results using equation (3).

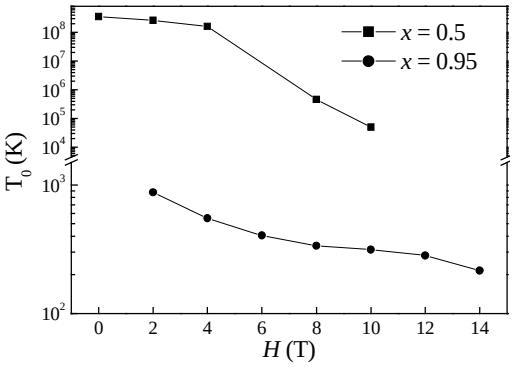

Fig. 7. The magnetic field dependencies of T_0 for $x = 0.5$ and $x = 0.95$.

In conclusion, we report the results of comprehensive magneto-transport property study for the high Ca concentration range of perovskite $La_{1-x}Ca_xMnO_3$ ($0.5 \le x < 1$). Especially it is found that the field dependence of $T_{\rm CO}$ obeys the formula $T_{\rm CO}/T_{\rm max} = 1 - a(n_{\rm Mn^{4+}} - n_0)^2$. For $x = 0.65$, $T_{\rm CO}$ arrives the maximum value 249.5 K in zero magnetic field, while the charge ordered (CO) state is most stable around $x = 0.75$. We also discussed the transport mechanism for $x = 0.5$ and 0.95 using the phase separation theory.

This work was supported by National Natural Science Foundation of China and the Ministry of Science and Technology of China.

References

1. C. Zener, Phys. Rev. **82**, 403 (1951).
2. S.W. Cheong, H.Y. Hwang, contribution to *Colossal Magnetoresistance Oxides, Monographs in Condensed Matter Science*, edited by Y. Tokura (Gordon Breach, London, 1999).

3. O. Toulemonde, F. Studer, A. Barnabe, B. Raveau, J.B. Goedkoop, Eur. Phys. J. B **18**, 233 (2000).
4. O. Toulemonde, F. Studer, A. Barnabe, A. Maignan, C. Martin, B. Raveau, Eur. Phys. J. B **4**, 159 (1998).
5. X.-G. Li, H. Chen, C.F. Zhu, H.D. Zhou, R.K. Zheng, J.H. Zhang, Appl. Phys. Lett. **76**, 1173 (2000).
6. J. Sichelschmidt, M. Paraskevopoulos, T. Brando, R. Wehn, D. Ivannikov, F. Mayr, K. Pucher, J. Hemberger, A. Pimenov, von Nidda HAK, P. Lunkenheimer, V.Y. Ivanov, A.A. Mukhin, A.M. Balbashov, A. Loidl, Eur. Phys. J. B **20**, 7 (2001).
7. E.O. Wollan, W.C. Koehler, Phys. Rev. **100**, 545 (1955).
8. C.H. Chen, S.W. Cheong, Phys. Rev. Lett. **76**, 4042 (1996).
9. P.G. Radaelli, D.E. Cox, M. Marezio, S.W. Cheong, Phys. Rev. B **55**, 3015 (1997).
10. S. Mori, C.H. Chen, S.W. Cheong, Phys. Rev. Lett. **81**, 3297 (1998).
11. G. Papavassiliou, M. Fardis, M. Belesi, M. Pissas, I. Panagiotopoulous, G. Kallias, D. Niarchos, C. Dimitropoulos, J. Dolinsek, Phys. Rev. B **59**, 6390 (1999).
12. J. Dho, I. Kim, S. Lee, K.H. Kim, H.J. Lee, J.H. Jung, T.W. Noh, Phys. Rev. B **59**, 492 (1999).
13. M. Roy, J.F. Mitchell, A.P. Ramirez, P. Schiffer, Phys. Rev. B **58**, 5185 (1999).
14. M. Roy, J.F. Mitchell, A.P. Ramirez, P. Schiffer, J. Phys. Cond. Matt. **11**, 4843 (1999).
15. M.R. Ibarra, J.M. De Teresa, contribution to *Colossal Magnetoresistance, Charge Ordering and Related Properties of Manganese Oxides*, edited by C.N.R. Rao, B. Raveau (World Scientific, Singapore 1998).
16. A.J. Mills, Nature **392**, 147 (1998).
17. Hiroyuki Fujishiro, Manabu Ikebe, Shuichi Ohshiden, Koshichi Noto, J. Phys. Soc. Jpn **69**, 1865 (2000).
18. A.P. Ramirez, P. Schiffer, S.W. Cheong, C.H. Chen, W. Bao, T.T. M. Palstra, P.L. Gammel, D.J. Bishop, B. Zegarski, Phys. Rev. Lett. **76**, 3188 (1996).
19. M.R. Presland, J.L Tollon, R.G. Buckley, R.S. Liu, N.E. Flower, Physica C **176**, 95 (1991).
20. S.D. Obertelli, J.R. Cooper, J.L. Tallon, Phys. Rev. B **46**, 14928 (1992).
21. N.F. Mott, E.A. Davis *Electronic Processes in Noncrystalline Materials* (Clarendon, Oxford, 1979).
22. J.M. De Teresa, M.R. Ibarra, P.A. Algarabel, C. Rltter, C. Marquina, J. Blasco, J. Garcia, A. Del Moral, Z. Arnold, Nature **386**, 256 (1997).
23. K.H. Kim, J.Y. Gu, H.S. Choi, G.W. Park, T.W. Noh, Phys. Rev. Lett. **77**, 1877 (1996).
24. G.M. Zhao, K. Conder, H. Keller, K.A. Muller, Nature **381**, 676 (1996).
25. A. Mills, P.B. Littlewood, B. I. Shraiman, Phys. Rev. Lett. **74**, 5144 (1995).
26. P. Schiffer, A.P. Ramirez, W. Bao, S.W. Cheong, Phys. Rev. Lett. **75**, 3336 (1995).